

# The performance of multiple datasets in characterizing the changes of extreme air temperature over China during 1979 to 2012

Lisuo Hu<sup>1,2</sup> · Gang Huang<sup>1,2,3</sup> · Kaiming Hu<sup>1,3,4</sup>

Received: 2 December 2016 / Accepted: 27 June 2017 / Published online: 8 July 2017  
© Springer-Verlag GmbH Austria 2017

**Abstract** Using multiple datasets, including three grid datasets (ERA-Interim, WFDEI, and SURF) and one station dataset, we analyzed the climatological distributions and trends of daily maximum air temperature (DMAT) and number of heat days (NHD) over China from 1979 to 2012. In general, all the three grid datasets show the highest climatological DMAT and NHD values in Xinjiang and southeast China, and increasing trends of DMAT and NHD in most of China. Nevertheless, both the climatological condition and trend exhibit differences in detail among the three grid datasets. Using the observed grid dataset (SURF) as a reference, the results show that the WFDEI dataset is closer to SURF than ERA-Interim in characterizing climatological features of DMAT and NHD, and the values from ERA-Interim dataset are lower than the SURF in most part of China. Since the trends of NHD in WFDEI are smaller than those in the other two grid datasets, especially in the middle and lower reaches of the Yangtze River, ERA-Interim is better than WFDEI in representing the trends of NHD. In four regions: Chuanyu, Huanghuai, Xinjiang, and Southeast where the NHD occurs frequently and increases rapidly, the WFDEI is more reliable than ERA-Interim due to the fact that the changes of regional NHD in WFDEI are more consistent with those

in observed datasets. Because there exist biases in the records of DMAT between the ERA-interim and WFDEI, it is better to adopt percentile index than absolute threshold to study the changes of China extreme air temperature when using reanalysis datasets.

**Keywords** Multiple datasets · Extreme air temperature · Root mean square difference · Trend differences

## 1 Introduction

The occurrence and change of extreme air temperature have attracted much attention globally because of their high impacts (Coumou and Rahmstorf 2012; Perkins et al. 2012; Zander et al. 2015; Zhao et al. 2016). Extreme air temperature events have significant influences on society and ecosystem, affecting the consumption of electricity and water, and inducing forest fires and crop losses (Peng et al. 2004; Coumou and Rahmstorf 2012). Besides, since prolonged exposure to extreme high air temperature could lead to heat-related illnesses, such as heat-stroke, heat exhaustion, heat cramps, and respiratory diseases (Luber and McGeethin 2008; Lu and Chen 2016), heat waves have disastrous consequences on occupational safety and human health (Robine et al. 2008; Kjellstrom et al. 2009; Dunne et al. 2013; Gu et al. 2016) and result in an increase of morbidity and mortality, especially in the elderly persons (Kilbourne 1997). The European heat wave in August 2003 caused more than 70,000 excess deaths, with 14,800 heat-related deaths in France alone (Bouchama 2004; Robine et al. 2008). In the more recent 2013 heat wave in eastern China, over 5600 heat-related illnesses were reported (Gu et al. 2016; Zhao et al. 2016). Comparing to the decade before (1991–2000), the number of deaths (136,000) due to heat waves increased rapidly (by 2300%) during the most recent decade (2001–2010), and the

✉ Gang Huang  
hg@mail.iap.ac.cn

<sup>1</sup> State Key Laboratory of Numerical Modeling for Atmospheric Sciences and Geophysical Fluid Dynamics, Institute of Atmospheric Physics, Chinese Academy of Sciences, Beijing 100029, China

<sup>2</sup> University of Chinese Academy of Sciences, Beijing 100049, China

<sup>3</sup> Joint Center for Global Change Studies, Beijing 100875, China

<sup>4</sup> Center for Monsoon System Research, Institute of Atmospheric Physics, Chinese Academy of Sciences, Beijing 100029, China

increase in deaths caused by heat events was much larger than the overall increase of 20% due to various extreme weather events including heat, cold, drought, storm, and floods (WMO 2013; Lu and Chen 2016).

Extreme air temperature weathers have become more frequent on the global scale under global warming (IPCC 2013). Climate models have projected an increasing trend in the frequency, intensity, and duration of air temperature extremes in the future (Kharin et al. 2007; Perkins et al. 2013). The changes of air temperature extremes over China exhibit significant spatial and temporal features. Recent researches indicated that extreme air temperature showed an increasing tendency throughout the country, especially in southeast China and Xinjiang province where the increasing values of heat days are more than 5 days/10 year (Wei and Chen 2009; Ding et al. 2010; Wang et al. 2012; Xu et al. 2013; Sun et al. 2014; Hu et al. 2016), while a weak decreasing trend which may partly due to the increasing of atmospheric aerosols and stratospheric temperature changes (Penner et al. 2004; Li et al. 2007; Yu and Zhou 2007) was identified in east central China. In addition, the details of trend show complex structures and regional characteristics, with the trend being dependent on the time period and the latitude of stations (Lu and Chen 2016). Some studies have suggested that the frequency of air temperature extremes showed a decadal variation with an obvious increase throughout the country since 1990s (Shi et al. 2009; Sun et al. 2011; Hu et al. 2016) and exhibited abrupt shifts in the 1990s (Qi and Wang 2012; Hu et al. 2016). Circulation anomalies are considered as a major factor affecting extreme heat, and the diversity and regional features of circulations should be emphasized (Lu and Chen 2016). Besides, high temperature extremes in China are affected by remote factors, including North Atlantic Oscillation (Sun 2012), Indian Ocean SST anomalies (Hu et al. 2012), and ENSO (Hu et al. 2013). Meanwhile, other studies indicate the impacts of underlying land surface on extreme temperature (Zhang et al. 2015).

Due to the complex structures and regional characteristics of the spatial and temporal features in extreme heat, the results are sensitive to the choice of datasets. Therefore, to improve the objectivity of results, it is important to choose a credible one among the various datasets before it could be used in analyzing the extreme air temperature. Previous studies indicated that each dataset has its own advantages and disadvantages, with inconsistent performances depending on the region, target period, and physical quantity, and there exist differences between various datasets to some extent (Huang 2006; Zhao and Fu 2006). However, there is lack of researches on comparison of datasets focusing on extreme heat events. For instance, Huang (2006) indicate that temperature at lower troposphere derived from ERA-40 is more reliable than from NCEP, and NCEP is more reliable than ERA-40 at upper troposphere. The objectives of present paper are to examine the performance of multiple datasets in characterizing the

changes of extreme air temperature over China with providing the spatial and temporal features of extreme air temperature among the various datasets and to examine the credibility of the two reanalysis datasets (ERA-Interim and WFDEI) with using the observed datasets as references in terms of the climatological features and trends of daily maximum air temperature (DMAT) and number of heat days (NHD).

## 2 Data and method

### 2.1 Meteorological data

The records of daily maximum air temperature are obtained from four datasets (three grid datasets and one station dataset) in present study, and the three grid datasets have a  $0.5^\circ \times 0.5^\circ$  horizontal resolution (equal to  $55 \times 55$  km approximately) covering the China region. Due to the fact that two reanalysis datasets (WFDEI and ERA-Interim) are available from 1979 forward, the present study mainly focuses on the period 1979–2012. The details of these datasets are introduced as follows.

The ERA-Interim is the global atmospheric reanalysis produced by the European Centre for Medium-Range Weather Forecasts (ECMWF) and has substantial improvements compared to ERA-40 in many aspects, such as the representation of the hydrological cycle, the quality of the stratospheric circulation, and the consistency in time of the reanalysis fields (Dee et al. 2011).

The WATCH-Forcing-Data-ERA-Interim (WFDEI) climate dataset (Weedon et al. 2014) is generated by applying bias correction to the ERA-Interim reanalysis product (Dee et al. 2011), following the same methodology implemented for a widely used WATCH Forcing Data (WFD) (Weedon et al. 2011). This dataset has the advantage of a high spatio-temporal resolution and a wide use for land surface modeling forcing (Zhao et al. 2015).

The China surface temperature grid dataset (SURF) is collected and processed by National Meteorological Information Center (NMIC) of the China Meteorological Administration (CMA). This dataset is obtained by spatial interpolation based on 2472 national stations over China, using the Thin Plate Spline (TPS) and combining with 3D geographical information. Therefore, it is reasonable to consider this dataset as a reference when examining the credibility of the reanalysis datasets (ERA-Interim and WFDEI).

In Sect. 3 and Sect. 4, we analyze the DMAT and NHD only based on the three grid datasets, which are conducive to quantitative comparison with serving the SURF dataset as a reference. In Sect. 5, we use the station dataset as well, which is derived from NMIC of CMA, for authentication, and the temperature was recorded according to the standard observation rules for China. The observed values are quality controlled using the NMIC conventional procedures, including

the climatological limit check, the station or regional extremes check, the internal consistency check, the temporal and spatial consistency checks, etc. (Li et al. 2009; Xu et al. 2013). The year with no missing values is judged as available, and a station with 30 or more available years during 1979 to 2012 is adopted in this analysis.

## 2.2 Methods

Present investigation chose two widely used indicators to characterize the extreme air temperature: absolute threshold and percentile index. CMA considers 35 °C of DMAT as a threshold to define extreme air temperature (absolute threshold). DMAT from 1981 to 2010 in June, July, and August are ranked in an ascending order, and then, the 90th percentile is chosen from the order as the percentile threshold (percentile index). The day when DMAT exceeds the threshold is defined as a heat day, and the number of heat days (NHD) is analyzed emphatically in present study.

## 3 The climatological condition and trend of DMAT

The climatological condition of DMAT in summer from 1981 to 2010 derived from three grid datasets is shown in Fig. 1a–c. Spatial patterns for the climatological conditions of DMAT among the three grid datasets are generally similar to each other, with high values (more than 30 °C) over Xinjiang province, Chuanyu area, and southeast China, and low values (less than 25 °C) in the Qinghai-Tibet Plateau and northeast China. Pattern correlation coefficients among three grid datasets are high, with 0.992 between ERA-Interim and SURF, 0.996 between WFDEI and SURF, and 0.995 between ERA-Interim and WFDEI. Since the SURF dataset is interpolated from high-resolution observed dataset directly, it features more regional characters than the other two reanalysis datasets (ERA-Interim and WFDEI).

Figure 1d–f shows the root mean square difference (RMSD) between ERA-Interim and SURF, between WFDEI and SURF, and between ERA-Interim and WFDEI, respectively. There is a common feature to note. The distribution of RMSD shows obvious east-west characteristics, with high values in western China and low values in eastern China basically. It indicates that the DMAT among datasets are diverse largely in the western China and consistent in the eastern China. If we consider that the DMAT record in SURF dataset is true, the DMAT record in WFDEI and EAR-Interim exists significant errors in the western China. And we found that the RMSD between WFDEI and SURF are smaller than those between ERA-Interim and SURF, with values less than 2.0 in most of regions throughout the country, suggesting that the DMAT records in WFDEI is relatively better than EAR-Interim.

Figure 2a–c displays the trends of DMAT during 1979 to 2012 obtained from ERA-Interim, WFDEI, and SURF. The DMAT increases almost in all the country, with higher values in northern China than southern China, and in inland than coastal regions. Increasing rate of DMAT is more than 0.6 °C/10 years in most parts of northern China and lower than 0.2 °C/10 years in southern China except for the Yangtze River Basin where the trends are significantly larger than surrounding regions. In detail, the trends of DMAT derived from ERA-Interim are higher over most regions, especially in northern China, while the tendency obtained from WFDEI is lower compared to the other two datasets (ERA-Interim and SURF) over middle and lower reaches of the Yangtze River and exhibits a weak decreasing trend over Guangxi province. Pattern correlation coefficients of the trends are 0.90 between ERA-Interim and SURF, 0.91 between WFDEI and SURF, and 0.87 between ERA-Interim and WFDEI. The result shows that WFDEI is slightly better than EAR-Interim in capturing the trends of DMAT over China.

To assess the significance of trend differences between datasets, we calculate the difference from two time series of DMAT from two datasets:  $d(t) = x(t) - y(t)$ , and then determine whether the trend in  $d(t)$  is significantly different from zero (Santer et al. 2000). The details of this approach applied to present study are illustrated as follows:

$$d_{ERA-SURF} = e(t) - s(t) \quad (1)$$

$$d_{WFDEI-SURF} = w(t) - s(t) \quad (2)$$

$$d_{ERA-SURF} = e(t) - w(t) \quad (3)$$

The  $e(t)$ ,  $w(t)$ , and  $s(t)$  are the time series of DMAT derived from ERA-Interim, WFDEI, and SURF; and  $d_{ERA-SURF}$ ,  $d_{WFDEI-SURF}$ ,  $d_{ERA-SURF}$  are the time series of difference between ERA-Interim and SURF, WFDEI and SURF, and ERA-Interim and SURF, respectively.

Figure 2d–f shows the trends of difference between ERA-Interim and SURF, WFDEI and SURF, and ERA-Interim and SURF. The trends of  $d_{ERA-SURF}$  (Fig. 2d) display that regions passing the test of statistical significance are mainly located in Xinjiang province, eastern Tibet, and coastlands. This indicates that the trends of DMAT obtained from ERA-Interim and SURF have significant discrepancies over these regions and are generally consistent over the other areas. As Fig. 2e shows, the areas where the trend of  $d_{WFDEI-SURF}$  exceeds the 95% significance level are scattered and the values of trend are small basically, illustrating that the trends of DMAT derived from WFDEI and SURF have similar values. Figure 2f manifests that the trends of DMAT calculated from ERA-Interim and WFDEI exhibit obvious deviation over mid-western China and coastal regions.

The above comparisons show that the results derived from WFDEI are more consistent with SURF than ERA-Interim.

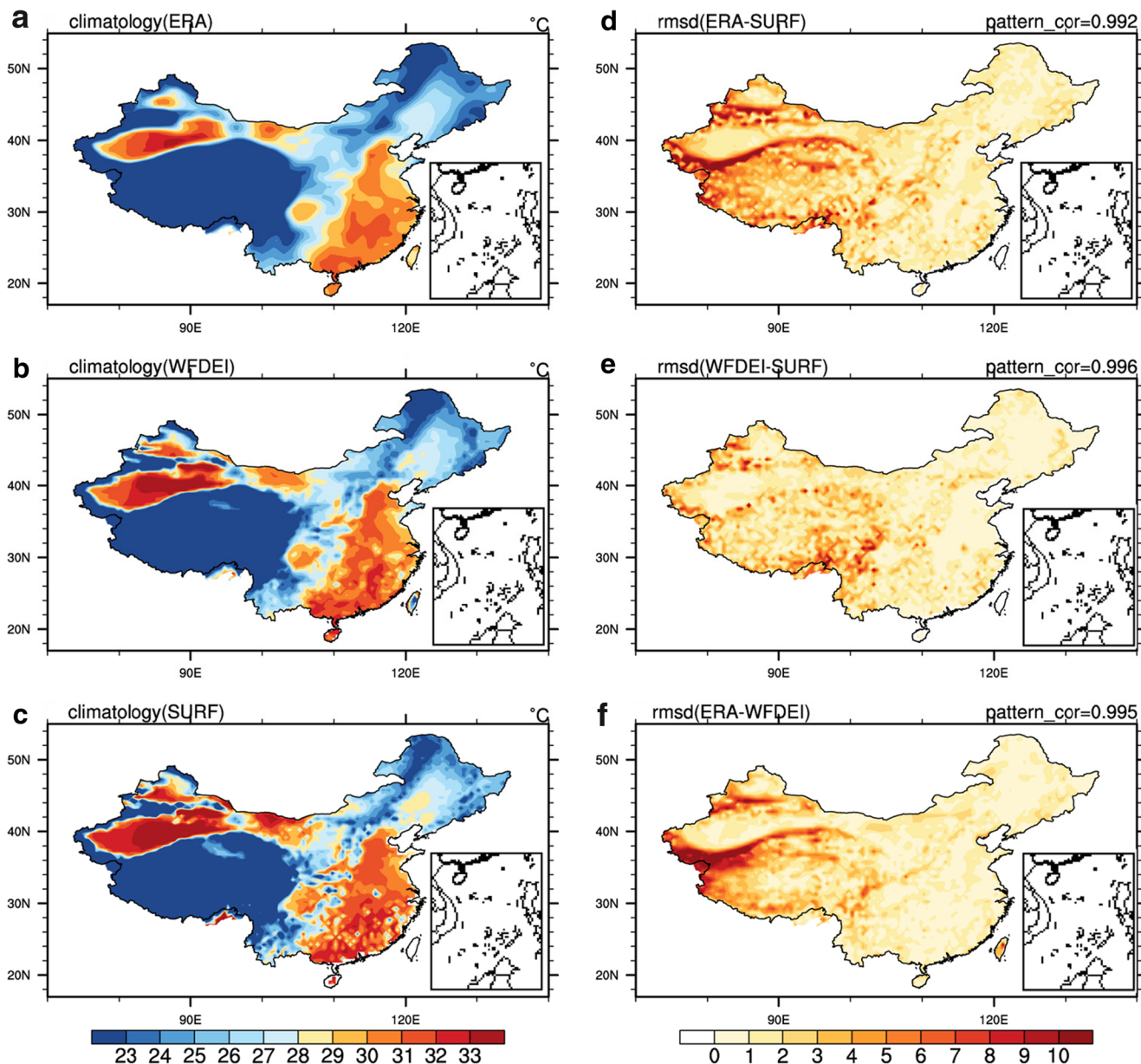


**Fig. 1** The climatological distribution (unit: °C) of DMAT during 1981 to 2010 obtained from **a** ERA-Interim, **b** WFDEI, and **c** SURF, and the root mean square difference (RMSD) of DMAT between ERA-Interim and SURF (**d**), WFDEI and SURF (**e**), and ERA-Interim and WFDEI (**f**), respectively

Thus, WFDEI is better than ERA-Interim to capture the climatological condition and tendency of DMAT from comprehensive comparisons.

## 4 The climatological condition and trend of NHD

### 4.1 Climatological condition

The present study adopts absolute threshold (35 °C) and percentile threshold (90 percentile of DMAT from 1981 to 2010 in summer) to define the heat day. The climatological distributions of NHD based on absolute threshold during 1981 to 2010 obtained from ERA-Interim, WFDEI, and SURF are

displayed in Fig. 3a–c. Spatial patterns derived from three datasets are consistent with each other, with heat days that occur frequently over Xinjiang province and southeast China, but the values of NHD obtained from three datasets exhibit obvious differences. In comparison, the climatological values of NHD derived from ERA-Interim (Fig. 1a) are smaller than those from the other two datasets (WFDEI and SURF), especially in two regions—Xinjiang province and southeast China. In addition, Fig. 3c shows more detailed regional characteristics of NHD in SURF than in the other two reanalysis datasets (ERA-Interim and WFDEI), especially in southeast China. Pattern correlation coefficients are 0.71 between ERA-Interim and SURF, 0.85 between WFDEI and SURF, and 0.90 between ERA-Interim and WFDEI, respectively. Once again,

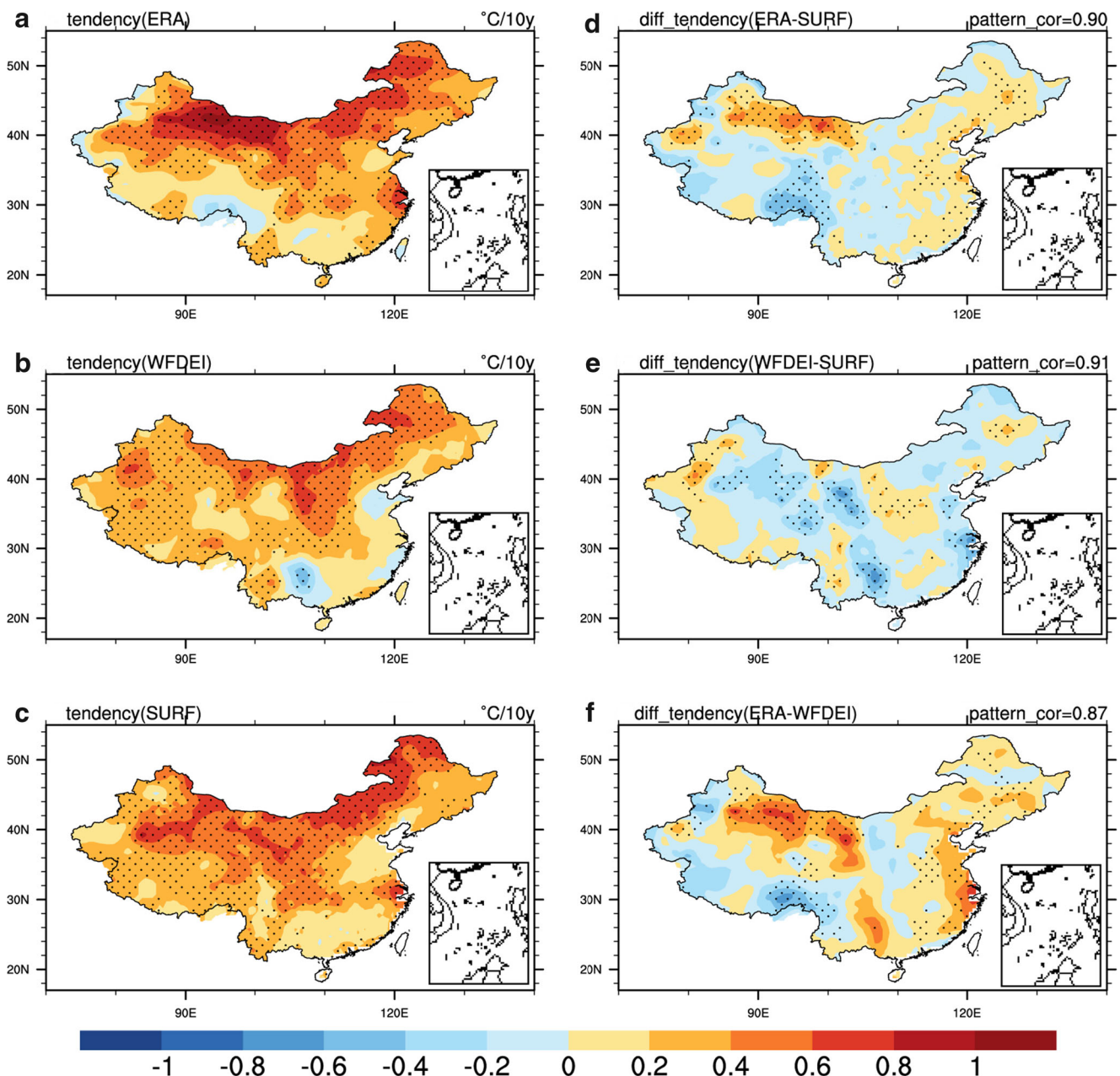


**Fig. 2** The trend (unit: °C/10y) of DMAT during 1979 to 2012 derived from **a** ERA-Interim, **b** WFDEI, and **c** SURF, and trend of difference time series between **d** ERA-Interim and SURF, **e** WFDEI and SURF, **f** ERA-

Interim and WFDEI. The point signs indicate grids exceed the 95% significance level

the WFDEI is better than ERA-Interim in recording the climatological conditions of NHD.

Figure 3d–f shows the root mean square difference (RMSD) between ERA-Interim and SURF, WFDEI and SURF, and ERA-Interim and WFDEI of NHD based on absolute threshold. A common feature is that the values of RMSD are large in the regions where heat days occur frequently, such as Xinjiang province and southeast China, indicating that the NHD based on absolute threshold is diverse largely over these regions among the three datasets. In comparison, RMSD calculated from two reanalysis datasets

(ERA-Interim and WFDEI) are the smallest (Fig. 3f), followed by WFDEI and SURF (Fig. 3e), while the values of RMSD derived from ERA-Interim and SURF are the largest (Fig. 3d).

Spatial patterns of the 90th percentile from DMAT (TX90) in summer from 1981 to 2010 calculated from ERA-Interim, WFDEI, and SURF are generally comparable (Fig. 4a–c), with high values in Xinjiang province and southeast China. In comparison, there are two major different features of TX90 between the three grid datasets. First, the values of TX90 obtained from ERA-Interim are smaller than WFDEI and SURF, especially over Xinjiang province and southeast

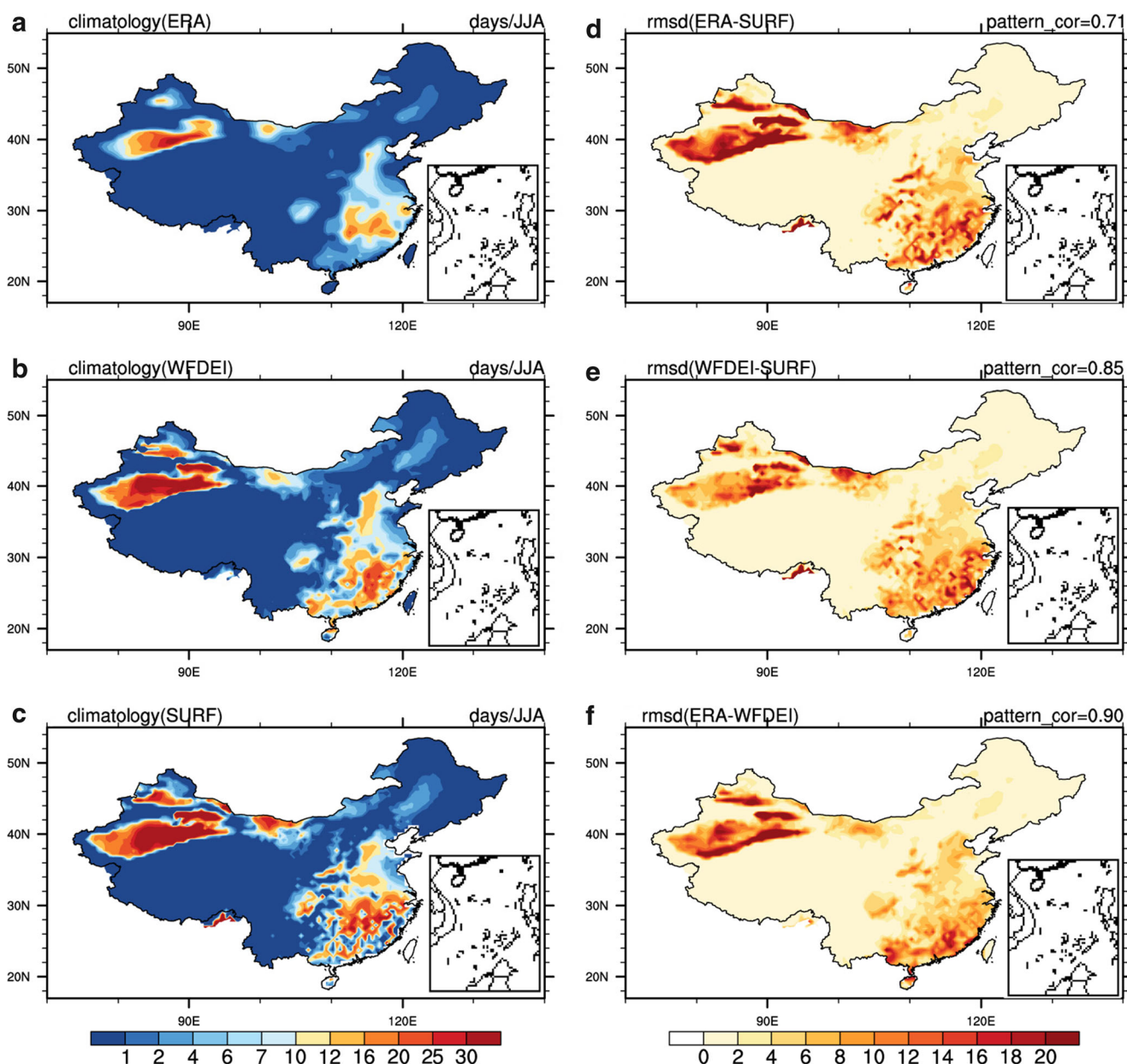


**Fig. 3** The climatological condition (unit: days/JJA) of number of heat days (NHD) based on absolute threshold during 1981 to 2010 obtained from **a** ERA-Interim, **b** WFDEI, and **c** SURF, and the root mean square

difference (RMSD) between ERA-Interim and SURF (**d**), WFDEI and SURF (**e**), and between ERA-Interim and WFDEI (**f**)

China. Second, the spatial distribution of TX90 derived from SURF displays distinct regional features, which are not apparent in two reanalysis datasets: ERA-Interim and WFDEI. Spatial pattern correlation coefficients of TX90 between the three datasets are larger than those based on absolute threshold, with 0.97 between ERA-Interim and SURF, 0.98 between WFDEI and SURF, and 0.98 between ERA-Interim and WFDEI.

The values of RMSD among the three grid datasets of NHD based on percentile index (Fig. 4d–f) are smaller than those based on absolute threshold generally. The RMSD is generally higher over the south China (south of 35° N) than

north China (north of 35° N), implying that NHD based on percentile index obtained from the three datasets is more consistent in north China than in south China.

From the values of pattern correlation coefficient and RMSD, the climatological conditions of NHD based on percentile index derived from the three grid datasets are more consistent than those based on absolute threshold, partly due to the existence of uniform bias in DMAT among the three grid dataset. In addition, the results obtained from WFDEI are more consistent with SURF than ERA-Interim, revealing that WFDEI is more credible than ERA-Interim in charactering the climatological conditions of NHD.

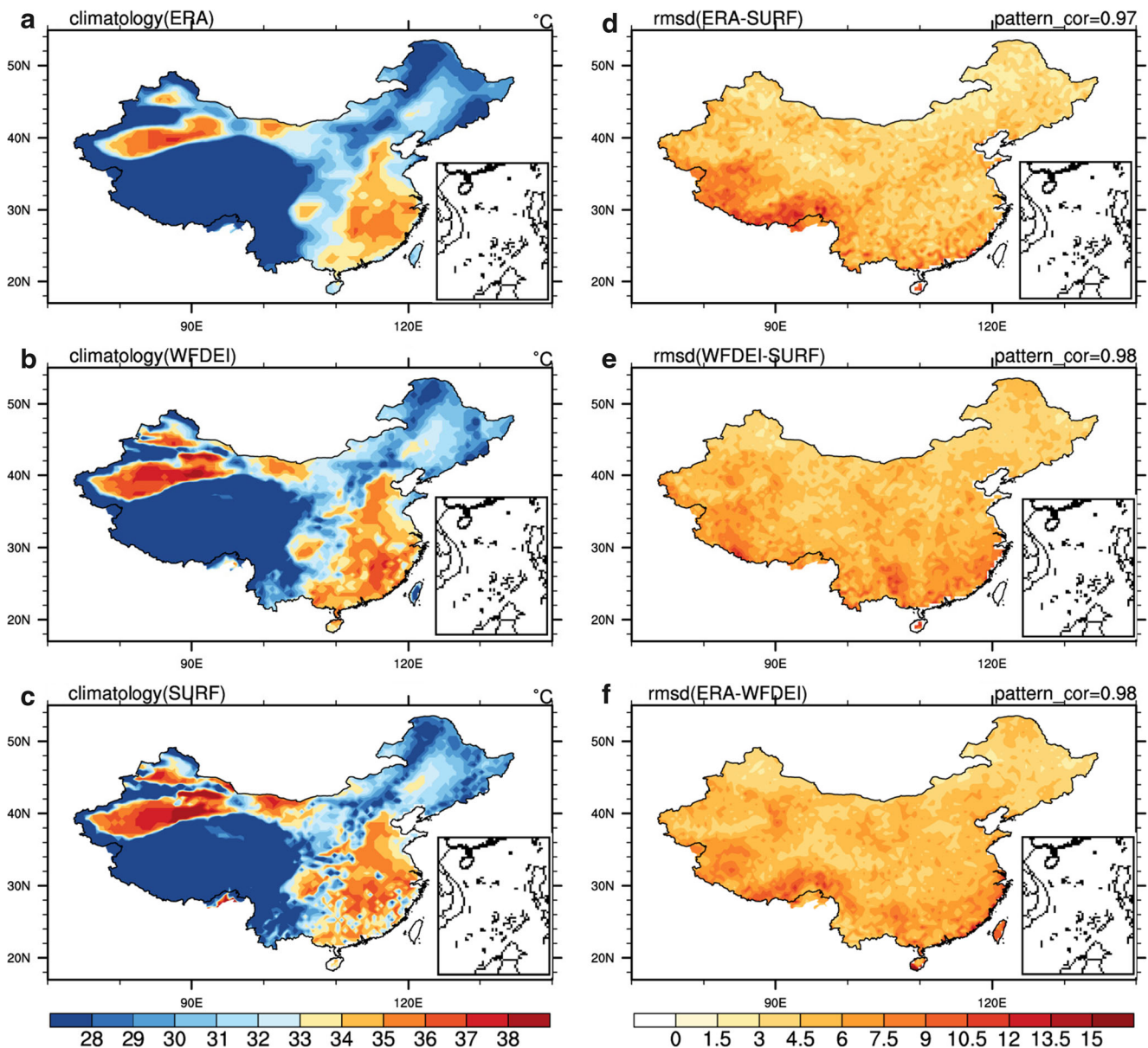


**Fig. 4** The 90 percentile of DMAT (unit: °C) in summer during 1981 to 2010 obtained from **a** ERA-Interim, **b** WFDEI, and **c** SURF, and the root mean square difference (RMSD) between ERA-Interim and SURF (**d**), WFDEI and SURF (**e**), and between ERA-Interim and WFDEI (**f**)

## 4.2 Trend

Figure 5a–c displays the trends of NHD based on absolute threshold from 1979 to 2012 obtained from ERA-Interim, WFDEI, and SURF. The NHD increased in most parts of China, especially over Xinjiang province and southeast China where the NHD increases by more than 3.0 days/10 years generally. From Fig. 5b, it can be clearly seen that the trends obtained from WFDEI are significantly smaller than those from the other two datasets (ERA-Interim and SURF), especially in middle and lower reaches of the Yangtze River, and have slight decreasing trends in Shandong and Guangxi province. Pattern correlation coefficients from the trends of

NHD based on absolute threshold are 0.74 between ERA-Interim and SURF, 0.71 between WFDEI and SURF, and 0.57 between ERA-Interim and WFDEI.

Using the method introduced in Sect. 3 to assess the significance of trend differences between datasets, the time series of difference ( $d_{ERA-SURF}$ ,  $d_{WFDEI-SURF}$ ,  $d_{ERA-WFDEI}$ ) for NHD based on absolute threshold are derived from ERA-Interim and SURF, WFDEI and SURF, and ERA-Interim and SURF, respectively; then, the trends of difference are calculated, which are shown in Fig. 5d–f. The regions where the trends of difference among the three datasets exceed 95% significance level are mainly observed in Xinjiang province. This reveals that a significant discrepancy exists in the trends of NHD obtained from the three

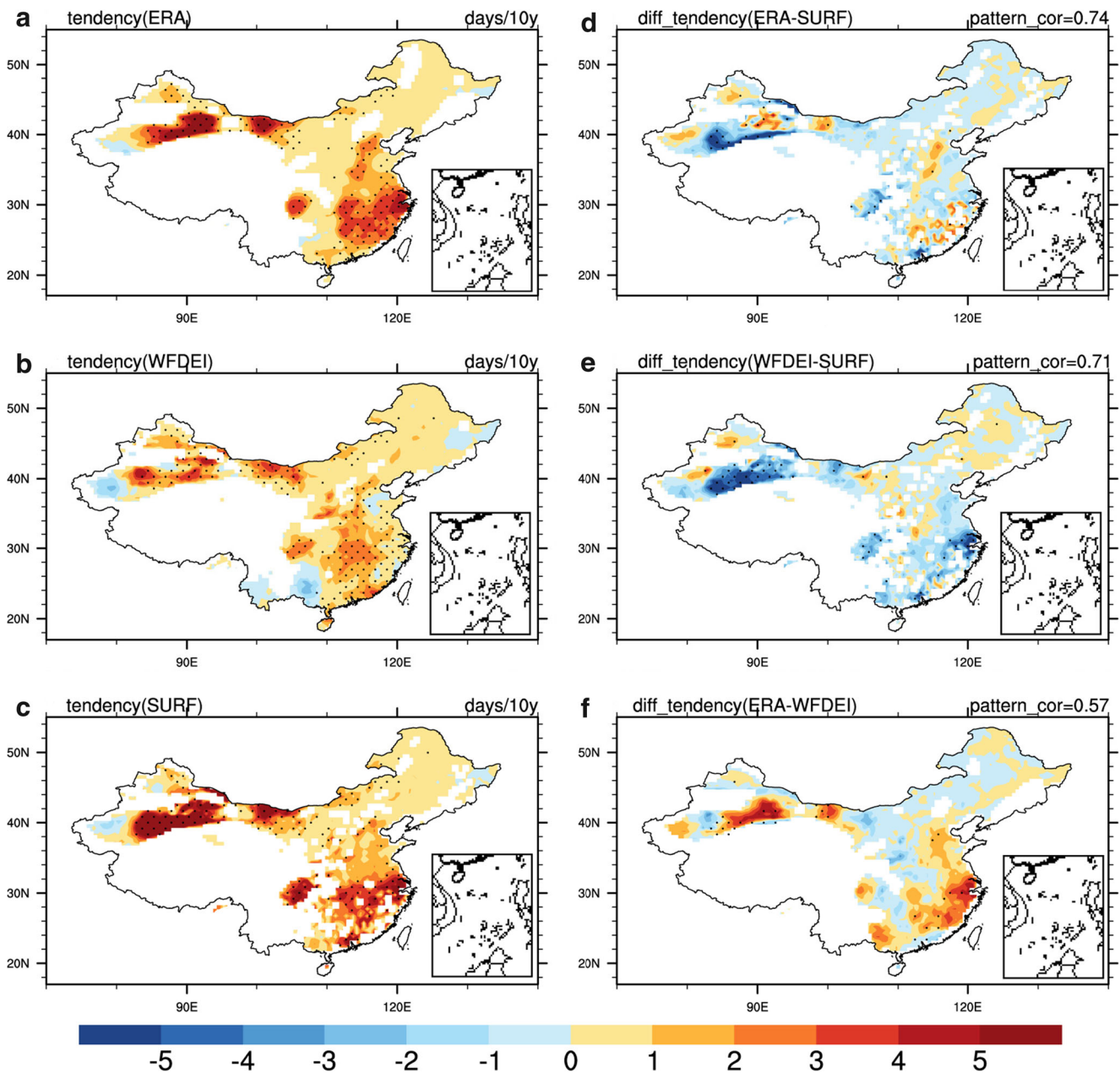


**Fig. 5** The trend (unit: days/10 years) of NHD based on absolute threshold during 1979 to 2012 derived from **a** ERA-Interim, **b** WFDEI, and **c** SURF, and trend of difference time series between **d** ERA-Interim

and SURF, **e** WFDEI and SURF, **f** ERA-Interim and WFDEI. The point signs indicate grids exceed the 95% significance level

datasets in Xinjiang province and the trends tend to be generally consistent in most parts of China.

The NHD based on percentile index increased throughout the country from 1979 to 2012, with most parts exceeding the 95% significance level (Fig. 6a–c). Compared with the trends of NHD based on absolute threshold, the increasing tendency based on percentile index is large. The regions where NHD increased most rapidly are mainly in north China from the two reanalysis datasets, and in central China from SURF. In comparison with WFDEI and SURF, the trends of NHD based on percentile index obtained from ERA-Interim are smaller in Tibet Plateau and are

larger in northwest China (Fig. 6a). From Fig. 6b, the values of trend calculated from WFDEI are smaller than those from the other two datasets (ERA-Interim and SURF) in most parts of China, and a decreasing tendency is identified over Guangxi province. Pattern correlation coefficients calculated from the trends of NHD based on percentile index are larger than those based on absolute threshold, with 0.81 between ERA-Interim and SURF, 0.79 between WFDEI and SURF, and 0.73 between ERA-Interim and WFDEI.

The trends of difference for NHD based on percentile index derived from ERA-Interim and SURF, WFDEI and SURF, and

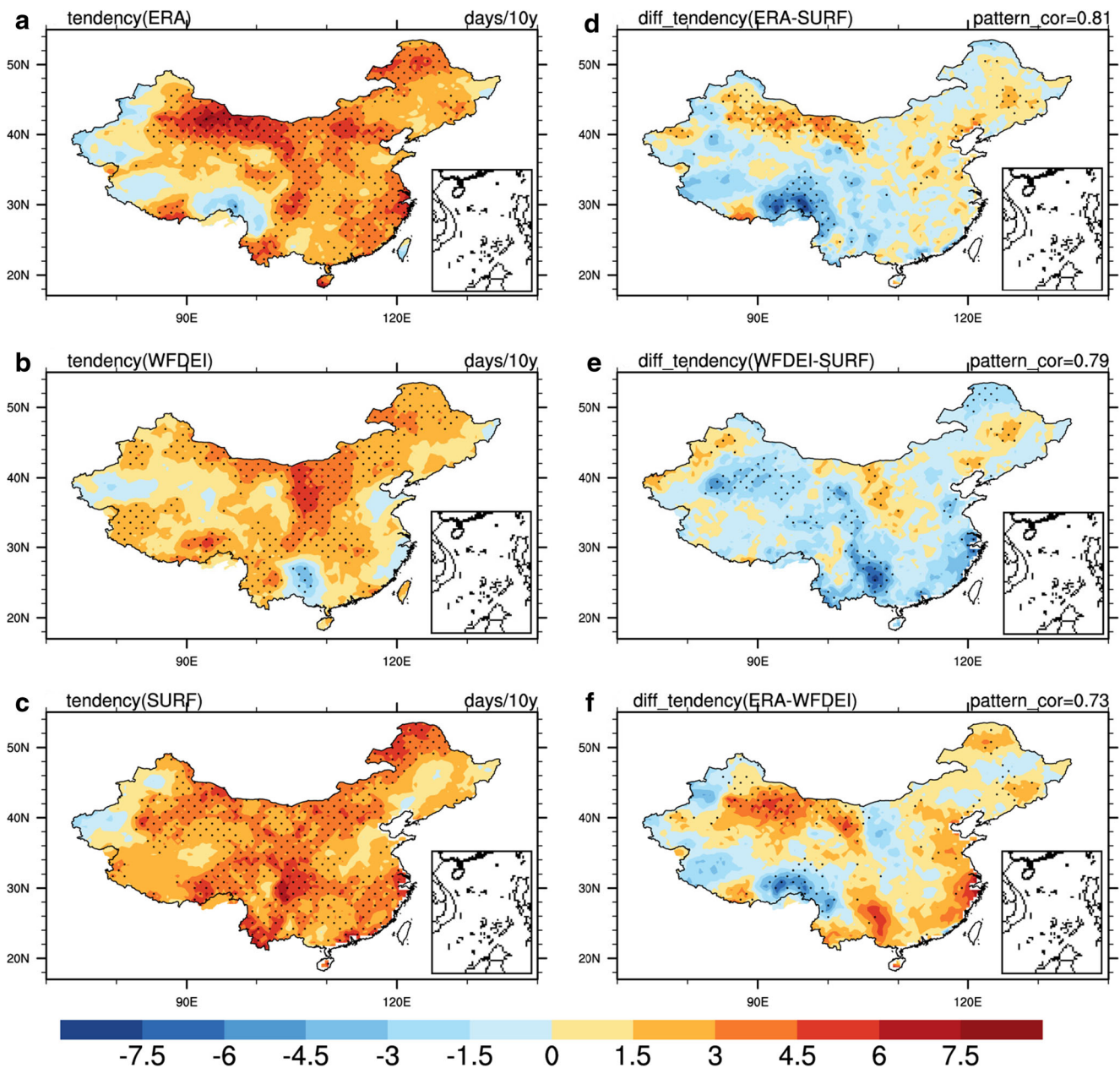


**Fig. 6** The same as Fig. 5 but based on percentile index

ERA-Interim and WFDEI are displayed in Fig. 6d–f. It can be concluded from the figures that the trends of NHD based on percentile index have significant differences in middle-west China between the three datasets, while they are generally consistent in eastern China.

Among the three grid datasets, the trends of NHD based on percentile index are more consistent than those based on absolute threshold, with the values of pattern correlation coefficients larger and trends of difference from time series among datasets smaller when based on percentile index. Since the trends of NHD based on two indices derived from WFDEI are smaller than ERA-Interim and SURF over middle and lower reaches of the Yangtze River, the spatial distribution of trends from ERA-

Interim is more consistent with SURF relatively, indicating that the ERA-Interim is better than WFDEI in discussing the trend features of heat days.

## 5 Variations of extreme air temperature in typical regions

According to the climatological distribution and trend of NHD based on two indices, four typical regions are chosen: Xinjiang region (75–92°E, 35–50°N), Huanghuai region (110–120°E, 30–38°N), Southern region (110–122°E, 22–30°N), and Chuanyu region (103–108°E, 28–33°N). The four

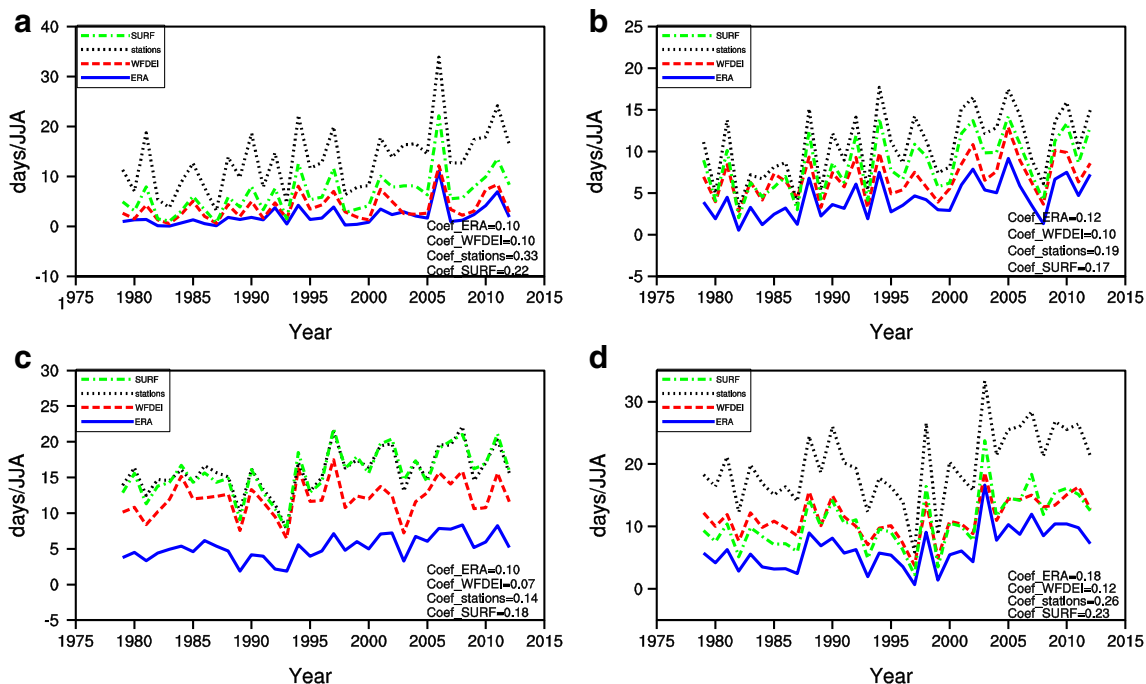
typical regions are the areas where the heat day occurs frequently and displays significant increasing trends. In addition to the three grid datasets, the analysis in this section includes the station dataset as well.

The changes of regional-averaged NHD based on absolute threshold from the four datasets over the Chuanyu, Huanghuai, Xinjiang, and Southern regions are shown in Fig. 7a–d. From Fig. 7a, the NHD over Chuanyu had little change from 1979 to late 1990s and increased rapidly since the late 1990s. Figure 7b, c indicates that the NHD over Huanghuai and Xinjiang maintained a steady increasing tendency during 1979 to 2012. The NHD over Southern region showed a slight decreasing trend from 1979 to late 1990s and a significant increasing trend after the late 1990s (Fig. 7d). Over the four typical regions, the NHD based on absolute threshold showed an increasing trend basically, but the details of change features exhibited regional characteristics. In comparison, the changes of regional averaged NHD display different features among the four datasets. First, the values of regional-averaged NHD derived from station dataset are obviously larger than those in the three grid datasets, especially over Chuanyu and Southern areas. Besides, over the four typical regions, linear trends of regional NHD during 1979 to 2012 from station datasets and SURF are larger than those from the two reanalysis datasets (ERA-Interim and WFDEI). Second, the variation features of

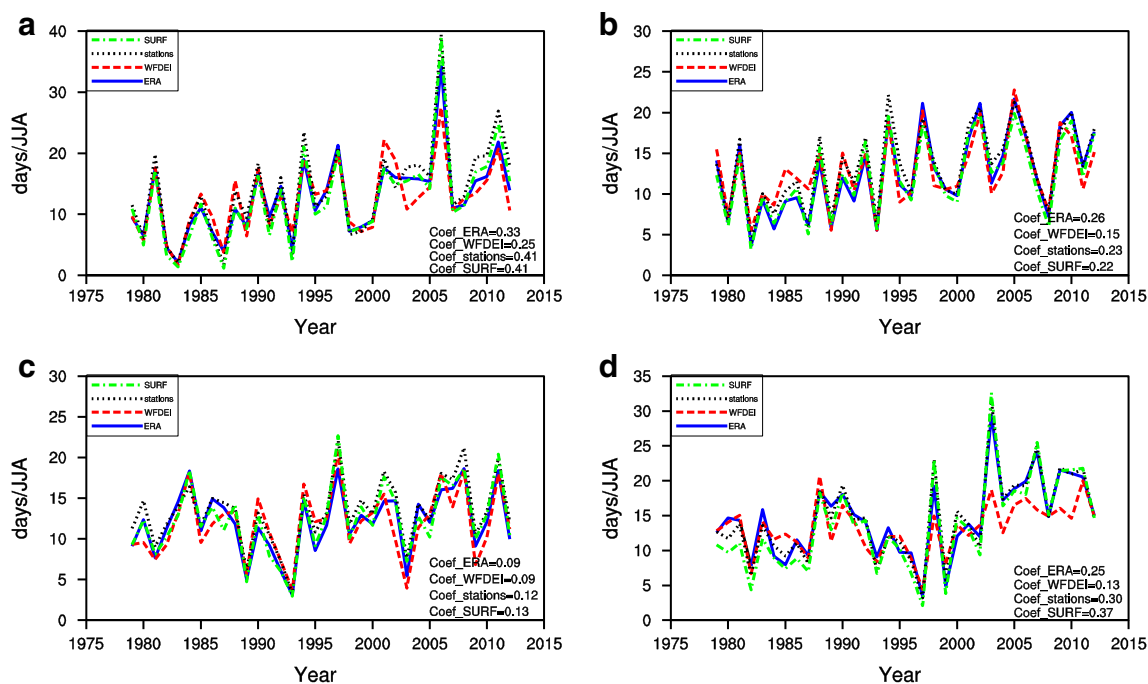
regional-averaged NHD derived from four datasets are consistent generally, with the correlation coefficients between four datasets all above 0.9. Third, from the two reanalysis datasets, the values of regional-averaged NHD calculated from WFDEI are closer to SURF and station dataset than ERA-Interim, especially in Xinjiang and Southern areas.

Figure 8a–d reveals the changes of the regional-averaged NHD based on percentile index during 1979 to 2012 derived from the four datasets in typical regions. The temporal features of NHD based on percentile index are consistent with that based on absolute threshold, with an increasing tendency generally. Basic coincidences are found among the curves calculated from the four datasets, indicating that the values and change features agree with each other among the datasets. However, the linear trends of regional-averaged NHD derived from station dataset and SURF are larger than those from ERA-Interim and WFDEI.

From the above comparisons, it can be concluded that the percentile index is a better choice than the absolute threshold in analyzing the regional changes of extreme air temperature from the reanalysis datasets, such as ERA-Interim and WFDEI. In addition, the values and temporal features calculated from WFDEI are more consistent with the observed datasets than those from the ERA-Interim, suggesting that WFDEI is better than ERA-Interim in charactering regional features in typical regions.



**Fig. 7** Changes of the regional NHD (unit: days/JJA) based on absolute threshold during 1979 to 2012 over **a** Chuanyu, **b** Huanghuai, **c** Xinjiang, and **d** Southern regions. The *black lines* depict station dataset, *blue lines* depict ERA-Interim, *red lines* depict WFDEI, *green lines* depict SURF



**Fig. 8** The same as Fig. 7 but based on percentile index

## 6 Discussions

Over mainland China on the whole, we have shown in the present study that DMAT and NHD have evidenced increasing trends, and global warming plays a key role in the variations of extreme temperature (Wei and Chen 2009). Else, both the black carbon produced by incomplete combustion (Ramanathan and Carmichael 2008) and increasing radiation associated with reduced clouds (Wild et al. 2005) contribute to warming and increasing of DMAT and NHD. Comparing with recent researches which focus on climatological condition and tendency of hot days and heat waves (Ding et al. 2010; Zhou and Ren 2011; Xu et al. 2013; Hu et al. 2016), the results in this paper are generally consistent with the finding in previous publications. The trends of DMAT and NHD here are generally a bit significant than those in the previous studies, and these differences mainly ascribed to the difference data processing methods used and time periods analyzed.

From the trend of NHD based on two indices, we found a weak decreasing trend in central China. The previous studies indicate that high temperature extremes in central China experienced a weak cooling trend during 1970s to early 1990s and a significant increasing trend since the middle 1990s (Wei and Chen 2009; Hu et al. 2016). There are two possible mechanisms contributing to this unexpectedly cooling trend. As most aerosols reflect sunlight to space and have a global cooling effect (Penner et al. 2004), the increasing of atmospheric aerosols in central China lead to a decreasing tendency of high temperature extremes to some extent. Yu and Zhou (2007) showed that the cooling trend in central China

connected to stratospheric temperature changes and interaction between the troposphere and stratosphere. As global warming continued to develop, the competition between regional cooling and global warming became biased toward the latter one, which then leads to the abrupt change in climate event extremes (Wei and Chen 2009).

According to the RMSD distributions and trends for differences between datasets, central-west parts of China are the major domains where most significant difference of results based on different datasets occurred. Since conventional observation is insufficient in central-west China, more unconventional observations are used in the reanalysis datasets. Biases are produced from assimilating unconventional datum including satellite and radar into reanalysis and other data processing. Else, the differences of results between datasets are more significant based on absolute index than percentile index, and this may be due to the biases in the records of DMAT between datasets.

A significant warming impact of urbanization on both mean and extreme temperature has been evaluated from previous studies (Zhou et al. 2004; Ren and Zhou 2014). The magnitudes of warming due to urbanization are different for daily maximum and daily minimum temperature and for different seasons, with stronger warming in winter and spring as opposed to summer, and larger increases in daily minimum temperature than daily maximum temperature (Wen Han et al. 2013; Ren and Zhou 2014; Sun et al. 2014). After providing some quantification of urbanization effect on summer temperatures, Sun et al. (2014) indicated that extreme summer heat is increasing with little urbanization effects. As present study

focuses upon daily maximum air temperature and warm days in summer over China, we did not eliminate the urbanization effect.

Although it is well known that grid datasets have no similar reliability as station datasets, there are no quality-controlled station datasets in some regions, such as desert areas and high-latitude localities. Thus, reanalysis datasets have to be chosen, and the present study can provide basis for selection of reanalysis datasets to some extent.

## 7 Summary

It is important to examine the performance of a dataset before it could be used in analyzing the spatial and temporal character of extreme air temperature in China. Using observed datasets as references, this study examines the climatological features and trends of daily maximum air temperature (DMAT) and number of heat days (NHD) in two widely used reanalysis datasets: ERA-Interim and WFDEI. The primary findings of the present study are as follows:

- (1) All the datasets show that the maximum climatological conditions of DMAT mainly occurred in Xinjiang province and Southeast China, and the DMAT increased almost in all of the China, with the largest trends in north China and decreasing gradually from north to south. The main discrepancy of climatological conditions of DMAT between the reanalysis datasets and observed datasets is found in the west China, and main biases for the trends of DMAT among the datasets mainly exist in west China and coastal regions. Moreover, we found that the results derived from WFDEI are more consistent with SURF than those from ERA-Interim, suggesting that the WFDEI is better than ERA-Interim in analyzing the spatial and temporal characters of DMAT in China.
- (2) We use two indices: the absolute threshold and percentile index to define the heat day. All the datasets show that Xinjiang and southeast China are two regions where heat days happened frequently. The NHD had an increasing tendency over the whole country, with high values in Xinjiang and southeast China based on absolute threshold and in north China and central China based on percentile index. The climatological values of NHD obtained from ERA-Interim are smaller than those from WFDEI and SURF, and there are significant differences in the trends of NHD in middle-west China among the three datasets, while the trends are generally consistent in eastern China. WFDEI is better in capturing the climatological features of NHD than ERA-Interim, and ERA-Interim is slightly better to characterize the trends of NHD. Besides, the climatological conditions and trend of NHD derived from the three grid datasets are more

consistent based on percentile index than those based on absolute threshold, with the values of pattern correlation coefficient larger and trends of difference from time series smaller based on percentile index.

- (3) According to the climatological distribution and trend of NHD based on the two indices, four typical regions are selected: Xinjiang (75–92°E, 35–50°N), Huanghuai (110–120°E, 30–38°N), Southern (110–122°E, 22–30°N), Chuanyu (103–108°E, 28–33°N). The NHD in the four regions displays an increasing trend with their respective regional features. Percentile index is a better choice when analyzing extreme air temperature over China based on reanalysis datasets as significant discrepancies are found between the reanalysis datasets and observed datasets based on absolute threshold. Besides, the WFDEI is better than ERA-Interim to analyze the variation features of regional NHD in the selected regions.

Results are sensitive to the choice of datasets due to the fact that discrepancies exist between the changes of DMAT and NHD derived from multiple datasets in various degrees, and present study exhibits the difference quantitatively. It can be concluded that WFDEI is more reliable than ERA-Interim in characterizing the spatial and temporal features of extreme air temperature from the comprehensive qualitative and quantitative analyses for DMAT and NHD over China. Besides, present study indicates that percentile index is a better choice when the features of extreme air temperature variations over China are obtained from reanalysis datasets.

**Acknowledgements** This research is supported by the National Natural Science Foundation of China (41425019 and 41661144016) and the public science and technology research funds projects of ocean (201505013).

## References

- Bouchama A (2004) The 2003 European heat wave. *Intensive Care Med* 30(1):1–3. doi:10.1007/s00134-003-2062-y
- Coumou D, Rahmstorf S (2012) A decade of weather extremes. *Nat Clim Chang* 2(7):491–496. doi:10.1038/nclimate1452
- Dee DP, Uppala SM, Simmons AJ, Berrisford P, Poli P, Kobayashi S, Andrae U, Balmaseda MA, Balsamo G, Bauer P, Bechtold P, Beljaars ACM, vande Berg L, Bidlot J, Bormann N, Delsol C, Dragani R, Fuentes M, Geer AJ, Haimberger L, Healy SB, Hersbach H, Holm EV, Isaksen L, Kallberg P, Koehler M, Matricardi M, AP MN, Monge-Sanz BM, Morcrette JJ, Park BK, Peubey C, de Rosnay P, Tavolato C, Thepaut JN, Vitart F (2011) The ERA-interim reanalysis: configuration and performance of the data assimilation system. *Q J R Meteorol Soc* 137(656):553–597. doi:10.1002/qj.493
- Ding T, Qian W, Yan Z (2010) Changes in hot days and heat waves in China during 1961–2007. *Int J Climatol* 30(10):1452–1462. doi:10.1002/joc.1989

- Dunne JP, Stouffer RJ, John JG (2013) Reductions in labour capacity from heat stress under climate warming. *Nat Clim Chang* 3(6): 563–566. doi:10.1038/nclimate1827
- Gu S, Huang C, Bai L, Chu C, Liu Q (2016) Heat-related illness in China, summer of 2013. *Int J Biometeorol* 60(1):131–137. doi:10.1007/s00484-015-1011-0
- Hu KM, Huang G, Qu X, Wu RG (2012) The impact of Indian ocean variability on high temperature extremes across the southern Yangtze River valley in last summer. *Adv Atmos Sci* 29(1):91–100
- Hu KM, Huang G, Wu RG (2013) A strengthened influence of ENSO on August high temperature extremes over the southern Yangtze Valley since the late 1980s. *J Clim* 26(7):2205–2221. doi:10.1175/jcli-d-12-00277.1
- Hu LS, Huang G, Qu X (2016) Spatial and temporal features of summer extreme temperature over China during 1960–2013. Theoretical and applied climatology. 1–13. doi: 10.1007/s00704-016-1741-x
- Huang G (2006) The assessment and difference of the interdecadal variations of climate change in northern part of China with the NCEP/NCAR and ERA-40 reanalysis data. *Clim Environ Res* 11(3):310–320
- IPCC (2013) The physical science basis contribution of working group I to the fifth assessment report of the intergovernmental panel on climate change. Cambridge University Press, Cambridge
- Kharin VV, Zwiers FW, Zhang X, Hegerl GC (2007) Changes in temperature and precipitation extremes in the IPCC ensemble of global coupled model simulations. *J Clim* 20(8):1419–1444. doi:10.1175/jcli4066.1
- Kilbourne EM (1997) Heat waves and hot environments. In: Noji EK (ed) In the public health consequences of disasters. Oxford University Press, New York, pp 245–269
- Kjellstrom T, Holmer I, Lemke B (2009) Workplace heat stress, health and productivity - an increasing challenge for low and middle-income countries during climate change. *Glob Health Action* 2: 46–51. doi:10.3402/gha.v2i0.2047
- Li LJ, Wang B, Zhou TJ (2007) Contributions of natural and anthropogenic forcings to the summer cooling over eastern China: an AGCM study. *Geophys Res Lett* 34:L18807. doi:10.1029/2007GL030541
- Li Q, Zhang H, Chen J, Li W, Liu X, Jones P (2009) A mainland China homogenized historical temperature dataset of 1951–2004. *Bull Am Meteorol Soc* 90(8):1062–1065. doi:10.1175/2009bams2736.1
- Lu RY, Chen RD (2016) A review of recent studies on extreme heat in China. *Atmos Ocean Sci Lett* 9(2):114–121
- Luber G, McGehee M (2008) Climate change and extreme heat events. *Am J Prev Med* 35(5):429–435. doi:10.1016/j.amepre.2008.08.021
- Peng SB, Huang JL, Sheehy JE, Laza RC, Visperas RM, Zhong XH, Centeno GS, Khush GS, Cassman KG (2004) Rice yields decline with higher night temperature from global warming. *Proc Natl Acad Sci U S A* 101(27):9971–9975. doi:10.1073/pnas.0403720101
- Penner JE, Dong XQ, Chen Y (2004) Observational evidence of a change in radiative forcing due to the indirect aerosol effect. *Nature* 427: 231–234
- Perkins SE, Alexander LV, Nairn JR (2012) Increasing frequency, intensity and duration of observed global heatwaves and warm spells. *Geophys Res Lett*. 39. doi:10.1029/2012gl053361
- Perkins SE, Pitman AJ, Sisson SA (2013) Systematic differences in future 20 year temperature extremes in AR4 model projections over Australia as a function of model skill. *Int J Climatol* 33(5):1153–1167. doi:10.1002/joc.3500
- Qi L, Wang Y (2012) Changes in the observed trends in extreme temperatures over China around 1990. *J Clim* 25(15):5208–5222. doi:10.1175/jcli-d-11-00437.1
- Ramanathan V, Carmichael G (2008) Global and regional climate changes due to black carbon. *Nat Geosci* 1(4):221–227. doi:10.1038/ngeo156
- Ren GY, Zhou YQ (2014) Urbanization effect on trends of extreme temperature indices of national stations over mainland China, 1961–2008. *J Clim* 27(6). doi:10.1007/JCLI-D-13-00393.1
- Robine JM, Cheung SLK, LeRoy S, Van Oyen H, Griffiths C, Michel JP, Herrmann FR (2008) Death toll exceeded 70,000 in Europe during the summer of 2003. *Comptes Rendus Biologies* 331(2):171–U175. doi:10.1016/j.crv.2007.12.001
- Santer BD, Wigley TML, Boyle JS, Gaffen DJ, Hnilo JJ, Nychka D, Parker DE, Taylor KE (2000) Statistical significance of trends and trend differences in layer-average atmospheric temperature time series. *J Geophys Res-Atmos* 105(D6):7337–7356. doi:10.1029/1999jd901105
- Shi J, Ding YH, Cui LL (2009) Climatic characteristics of extreme maximum temperature in east China and its causes. *Chin J Atmos Sci* 33(2):347–358
- Sun J (2012) Possible impact of the summer north Atlantic oscillation on extreme hot events in China. *Atmos Ocean Sci Lett* 5(3):231–234
- Sun J, Wang H, Yuan W (2011) Decadal variability of the extreme hot event in China and its association with atmospheric circulations. *Clim Environ Res* 16(2):199–208
- Sun Y, Zhang X, Zwiers FW, Song L, Wan H, Hu T, Yin H, Ren G (2014) Rapid increase in the risk of extreme summer heat in eastern China. *Nat Clim Chang* 4(12):1082–1085. doi:10.1038/nclimate2410
- Wang Z, Ding Y, Zhang Q, Song Y (2012) Changing trends of daily temperature extremes with different intensities in China. *Acta Meteorologica Sinica* 26(4):399–409. doi:10.1007/s13351-012-0401-z
- Weedon GP, Gomes S, Viterbo P, Shuttleworth WJ, Blyth E, Oesterle H, Adam JC, Bellouin N, Boucher O, Best M (2011) Creation of the WATCH forcing data and its use to assess global and regional reference crop evaporation over land during the twentieth century. *J Hydrometeorol* 12(5):823–848. doi:10.1175/2011jhm1369.1
- Weedon GP, Balsamo G, Bellouin N, Gomes S, Best MJ, Viterbo P (2014) The WFDEI meteorological forcing data set: WATCH forcing data methodology applied to ERA-interim reanalysis data. *Water Resour Res* 50(9):7505–7514. doi:10.1002/2014wr015638
- Wei K, Chen W (2009) Climatology and trend of high temperature extremes across China in summer. *Atmos Ocean Sci Lett* 2(3):153–158
- Wen Han QZ, Zhang XB, Xu Y, Wang B (2013) Detecting human influence on extreme temperature in China. *Geophys Res Lett* 40(6). doi: 10.1002/grl.50285
- Wild M, Gilgen H, Roesch A, Ohmura A, Long CN, Dutton EG, Forgan B, Kallis A, Russak V, Tsvetkov A (2005) From dimming to brightening: decadal changes in solar radiation at Earth's surface. *Science* 308:847–850. doi:10.1126/science.1103215
- WMO (2013) The global climate 2001–2010: A decade of climate extremes. WMO-No. 1103: 119pp. World Meteorological Organization, Switzerland
- Xu WQ, Wang XL, Yang S, Cao L, Feng Y (2013) Homogenization of Chinese daily surface air temperatures and analysis of trends in the extreme temperature indices. *J Geophys Res-Atmos* 118(17):9708–9720. doi:10.1002/jgrd.50791
- Yu RC, Zhou TJ (2007) Seasonality and three-dimensional structure of interdecadal change in the east Asian monsoon. *J Clim* 20:5344–5355. doi:10.1175/2007JCLI1559.1
- Zander KK, Botzen WJW, Oppermann E, Kjellstrom T, Garnett ST (2015) Heat stress causes substantial labour productivity loss in Australia. *Nature climate change*, 5(7): 647–+. doi: 10.1038/nclimate2623
- Zhang J, Liu ZY, Chen L (2015) Reduced soil moisture contributes to more intense and more frequent heat waves in northern China. *Adv Atmos Sci* 32:1197–1207. doi:10.1007/s00376-014-4175-3
- Zhao TB, Fu ZB (2006) Preliminary comparison and analysis between ERA-40, NCEP-2 reanalysis and observations over China. *Clim Environ Res* 11(1):14–32

- Zhao Y, Ducharne A, Sultan B, Braconnot P, Vautard R (2015) Estimating heat stress from climate-based indicators: present-day biases and future spreads in the CMIP5 global climate model ensemble. *Environ Res Lett*. doi:[10.1088/1748-9326/10/8/084013](https://doi.org/10.1088/1748-9326/10/8/084013)
- Zhao Y, Sultan B, Vautard R, Braconnot P, Wang HJ, Ducharne A (2016) Potential escalation of heat-related working costs with climate and socioeconomic changes in China. *Proc Natl Acad Sci U S A* 113(17):4640–4645. doi:[10.1073/pnas.1521828113](https://doi.org/10.1073/pnas.1521828113)
- Zhou YQ, Ren GY (2011) Changes in extreme temperature event frequency over mainland China, 1961–2008. *Clim Res* 50:125–139. doi:[10.3354/cr01053](https://doi.org/10.3354/cr01053)
- Zhou LM, Dickinson RE, Tian YH, Fang JY, Li QX, Kaufmann RK, Tucker CJ, Myneni RB (2004) Evidence for a significant urbanization effect on climate in China. *Proc Natl Acad Sci U S A* 101(26):9540–9544. doi:[10.1073/pnas.0400357101](https://doi.org/10.1073/pnas.0400357101)